SUPPLEMENTARY FIGURES

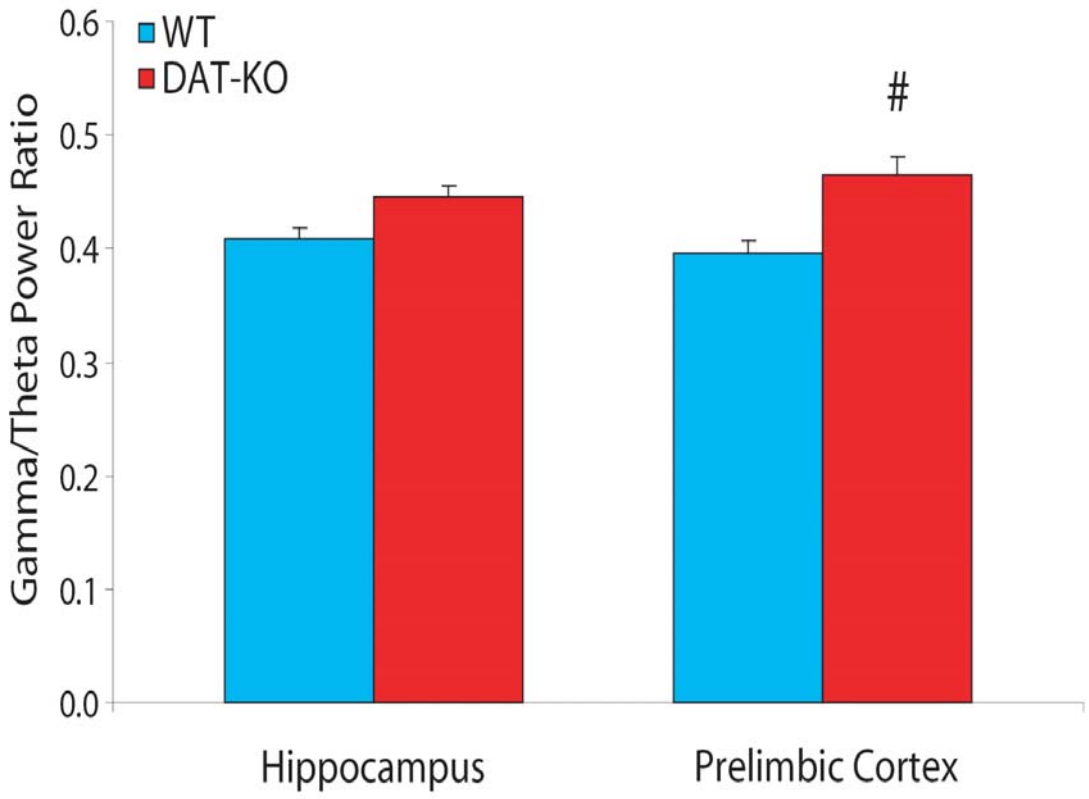

Supplementary Figure S1: Effect of persistent hyperdopaminergia on hippocampal and cortical gamma/theta power ratio in novelty exposed mice. There was no effect of genotype on the hippocampal Gamma/Theta ratio ($n = 40$ for both WT and DAT-KO LFP channels; $p > 0.05$, using One way ANOVA); however, the Gamma/Theta power ratio observed across prelimbic cortex was significant elevated in DAT-KO mice ($n = 40$ AND 37 for WT and DAT-KO LFP channels, respectively; $p < 0.001$, using One way ANOVA).

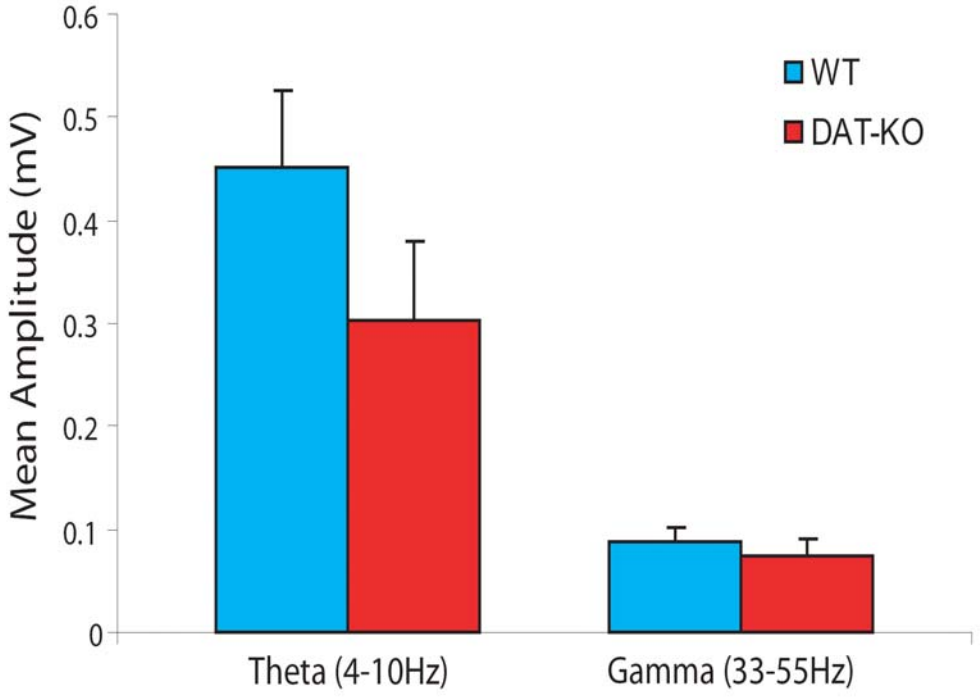

Supplementary Figure S2: Cortical theta and gamma oscillatory power in DAT-KO mice. DAT-KO mice displayed cortical theta and gamma oscillatory power that was statistically indistinguishable than that observed in WT mice; $p > 0.05$ using the students t-test.

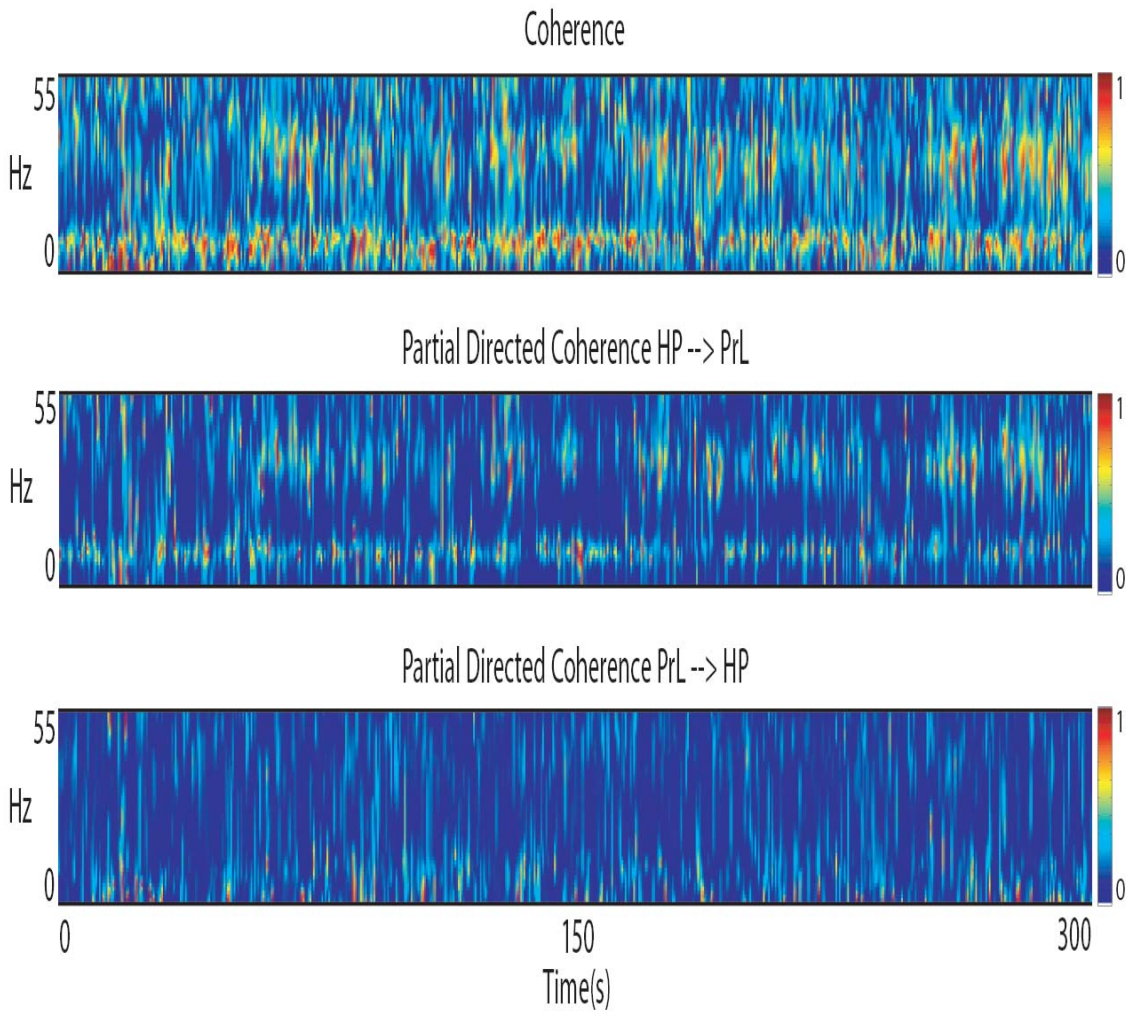

Supplementary Figure S3: Sample coherence and partial directed coherence plots determined for a WT mouse during a five minute period of active exploration.

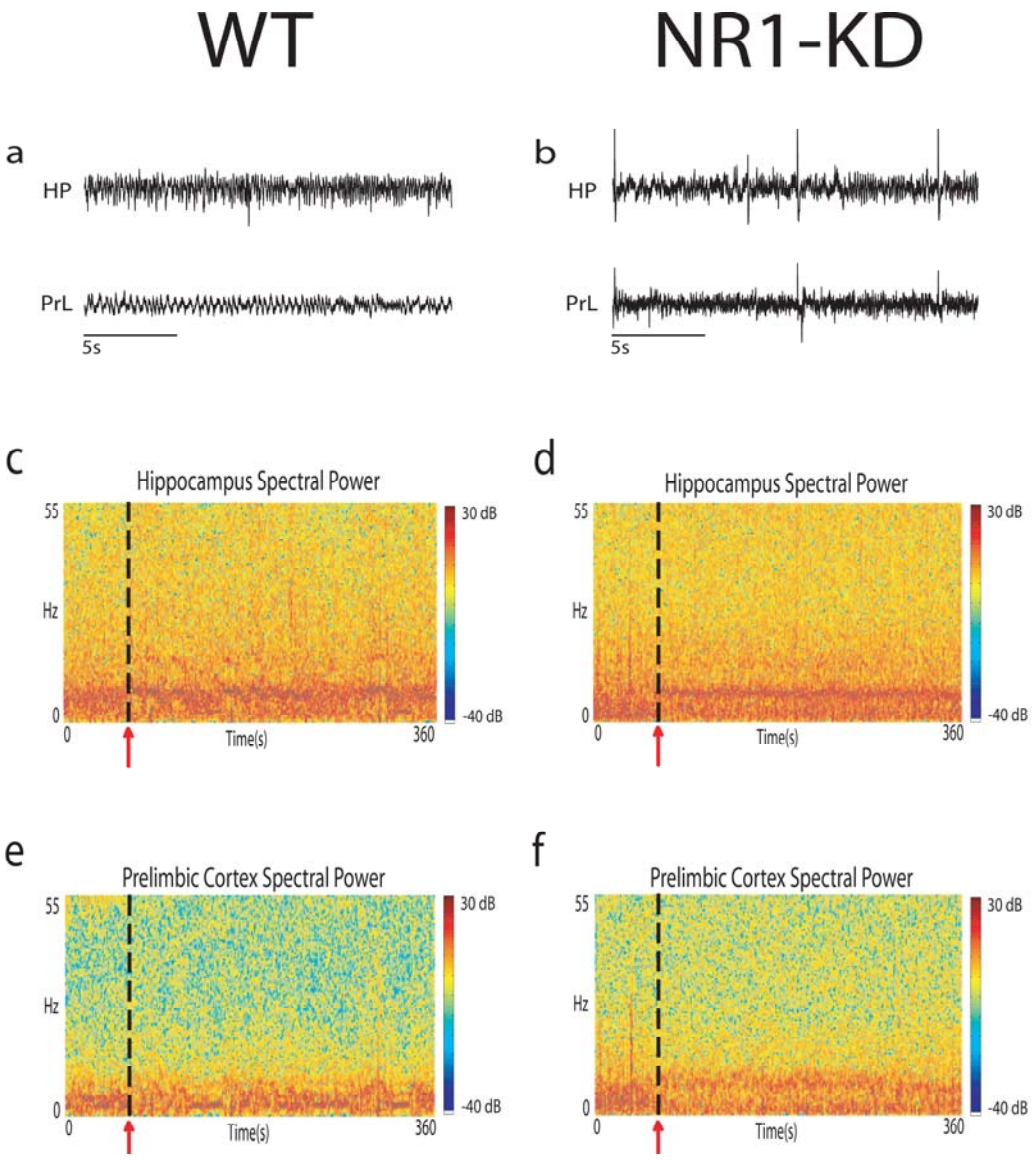

Supplementary Figure S4: Hippocampal and prelimbic cortical local field potential power spectra in WT and NR1-KD mice. **a-b**) LFP oscillations recorded from hippocampus and prelimbic cortex in a) WT and b) NR1-KD mice. NR1-KD mice displayed population firing events across the two brain areas that were consistent with seizure-like activity. This seizure-like activity was primarily observed while NR1-KD animals were in their home cage **c-d**) Hippocampal LFP power spectra recorded from c) WT and d) NR1-KD mice. Images depict power spectra recorded while animals were in their home cage (1 minute of data displayed) juxtaposed with LFP's recorded while animals explored a novel environment (5 minutes of data displayed, see red arrow). There was no significant effect of genotype or environment on the HP gamma/theta power ratio; n = 29 and 21, and 29 and 37 for hippocampal LFP channels recorded from WT and NR1-KD animals recorded in their home cage and the novel environment, respectively. **e-f**) Prelimbic cortex LFP power spectra recorded from e) WT and f) NR1-KD mice.

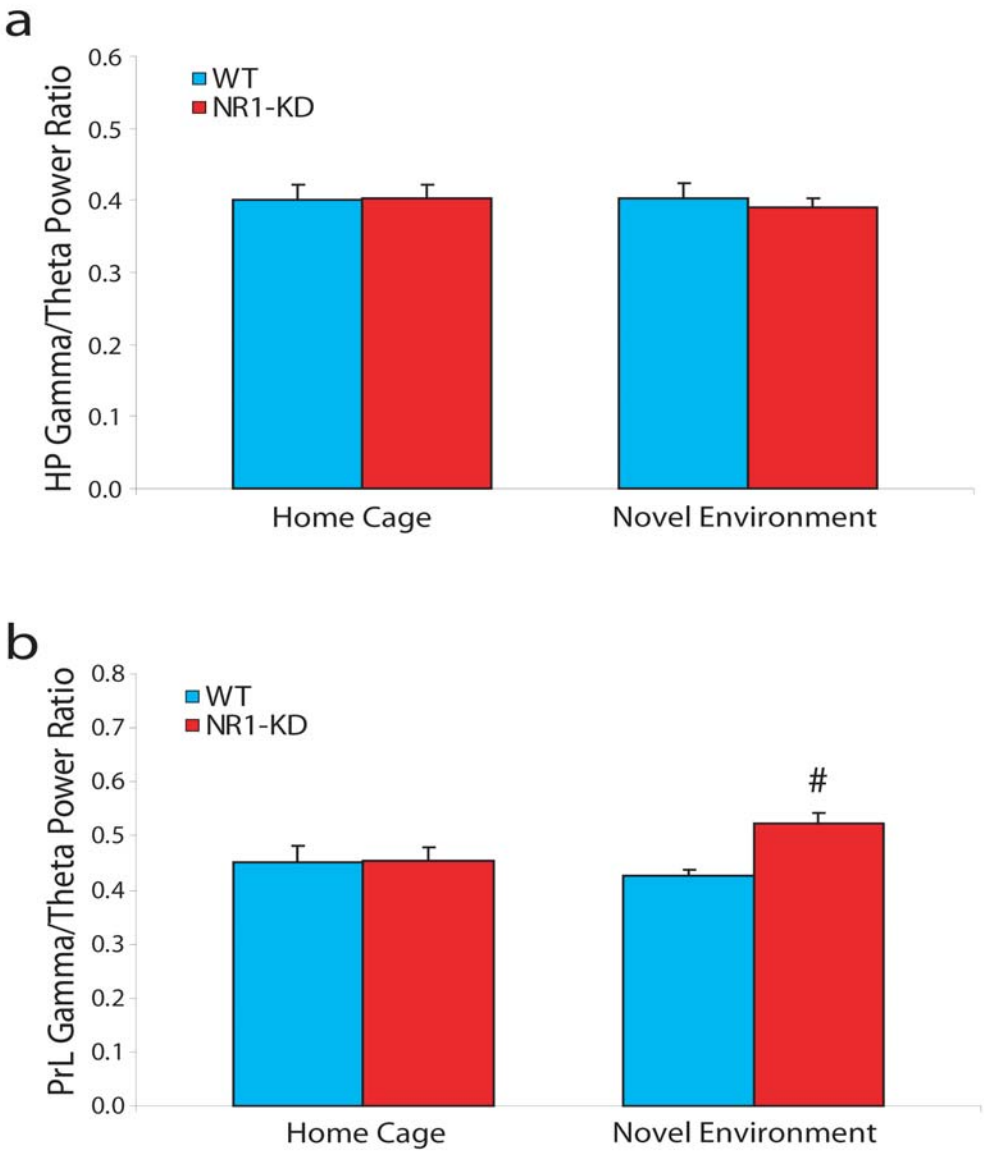

Supplementary Figure S5: Effect of NMDA receptor hypofunction and novelty on hippocampal and cortical gamma/theta power ratio. **a**) There was no effect of genotype or environment on the hippocampal (HP) Gamma/Theta ratio; Two-way ANOVA of Genotype x Environment; $p > 0.05$; n = 29 and 21, and 29 and 37 for HP LFP channels recorded from WT and NR1-KD animals recorded in their home cage and the novel environment, respectively. **b**) NR1-KD mice displayed a significantly higher Gamma/Theta power ratio in the novel environment compared to WT mice; Two-way ANOVA of Genotype; $p < 0.05$; # = $p < 0.05$ compared to WT animals in the same environment using the students t-test; n = 32 and 24, and 32 and 40 for PrL LFP channels recorded from WT and NR1-KD animals in their home cage and the exploring the novel environment, respectively.

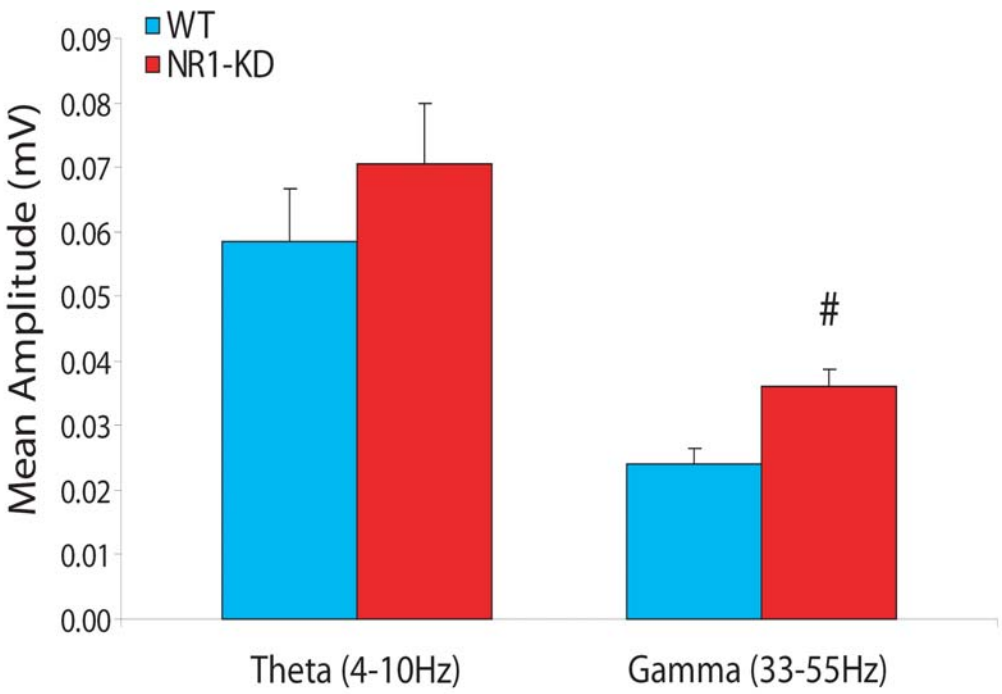

Supplementary Figure S6: Effect of chronic NMDA receptor hypofunction on cortical theta and gamma power during novelty exposure. There was no effect of chronic NMDA receptor hypofunction on cortical theta power (students t-test, $p > 0.05$); however, NR1-KD mice displayed significantly higher cortical gamma power following novelty exposure, compared to WT mice; # = $p < 0.05$ compared to WT animals in the same environment using the students t-test; n = 32, and 40 for PrL LFP channels recorded from WT and NR1-KD mice exploring the novel environment, respectively.

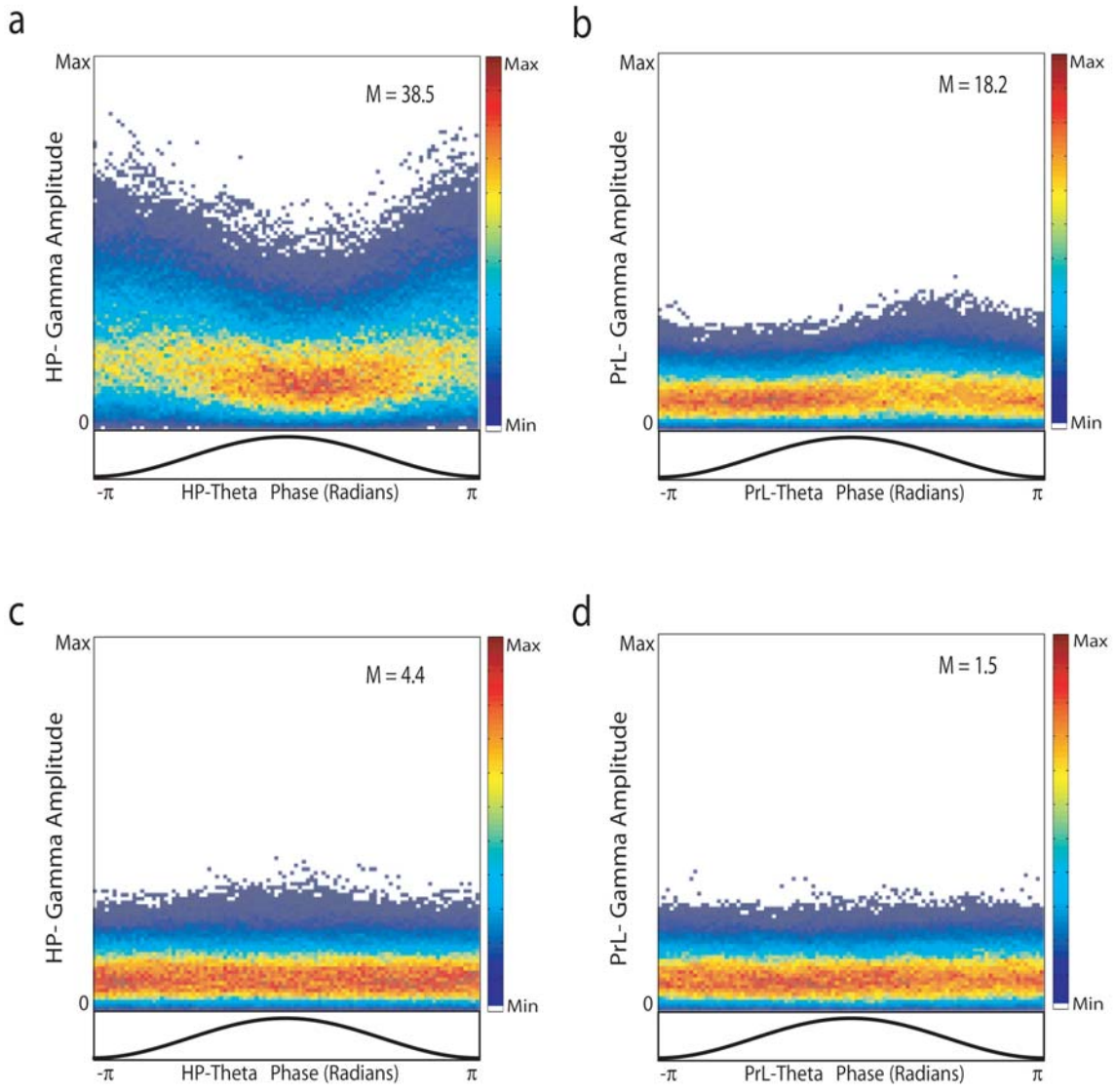

Supplementary Figure S7: Phasic modulation of prefrontal cortical and hippocampal gamma oscillations by theta oscillations. Sample two dimensional histograms of instantaneous theta phase values versus instantaneous gamma amplitude values recoded from **a-b**) WT and **c-d**) NR1-KD mice during 5 minutes of exploration in novel environment. WT mice displayed high cross frequency phase coupling across channels recorded from a) hippocampus (HP) and b) prelimbic cortex (PrL). NR1-KD mice displayed significantly diminished or absent cross frequency phase coupling across channels recorded from c) hippocampus and d) prelimbic cortex. The modulation index calculated for each channel is shown in the upper right corner of each histogram.

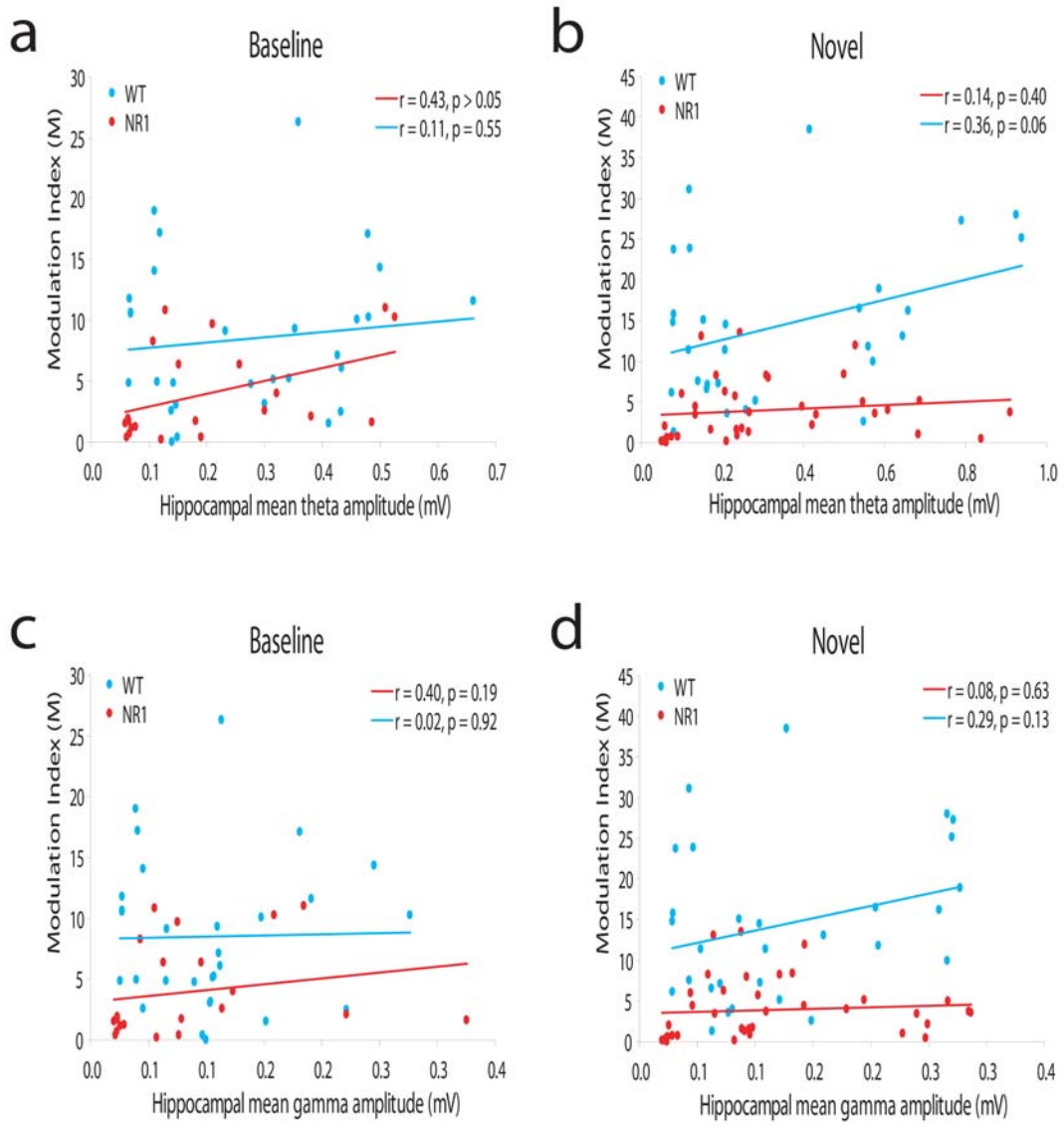

Supplementary Figure S8: The effect of hippocampal LFP oscillatory amplitude, novelty exposure, and persistent NMDA hypofunction on cross frequency phase coupling. The modulation index was not significantly correlated with the mean hippocampal theta or gamma amplitude in WT and NR1-KD mice in their home cage or exploring the novel environment. Importantly, tread lines predicted higher cross frequency phase coupling in WT animals for all theta and gamma oscillatory amplitudes.

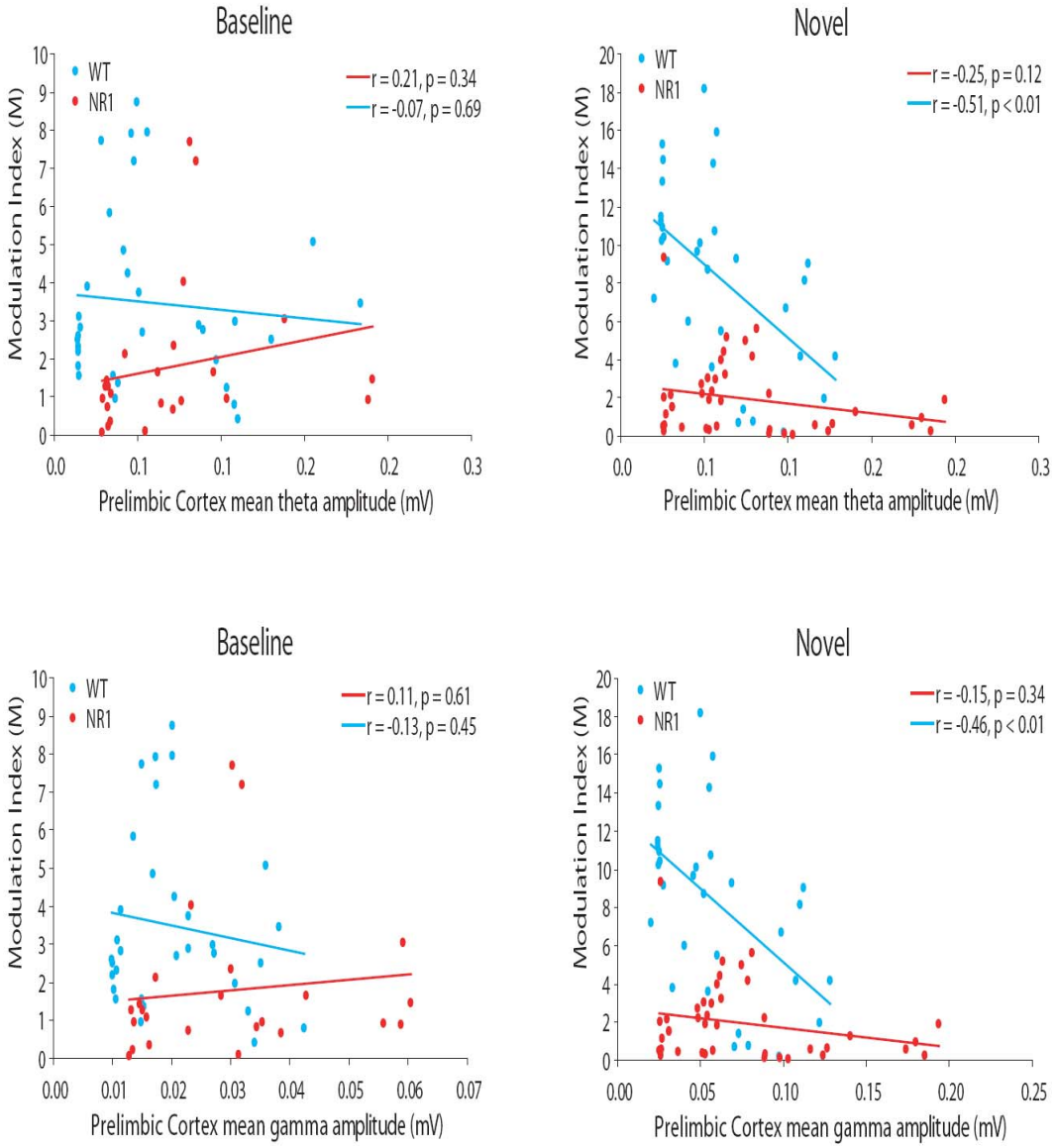

Supplementary Figure S9: The effect of prelimbic cortex LFP oscillatory amplitude, novelty exposure, and persistent NMDA hypofunction on cross frequency phase coupling. The modulation index was negatively correlated with the mean prelimbic cortex theta and gamma amplitude in WT mice exploring the novel environment, but not in their home cage. Additionally, the modulation index was not significantly correlated with the mean prelimbic cortex theta or gamma amplitude in NR1-KD mice in their home cage or exploring the novel environment. Importantly, tread lines predicted higher cross frequency phase coupling in WT animals for all theta and gamma oscillatory amplitudes.